Available online at www.sciencedirect.com
ScienceDirect
Journal of Nuclear Materials 367–370 (2007) 812–816
journal of nuclear materials
www.elsevier.com/locate/jnucmat

Effects of helium implantation on damage during pulsed high heat loading of tungsten

K. Tokunaga [a,*], T. Fujiwara [a], K. Ezato [b], S. Suzuki [b], M. Akiba [b], N. Yoshida [a]

[a] Research Institute for Applied Mechanics, Kyushu University, Kasuga, Fukuoka 816-8580, Japan
[b] Naka Fusion Institute, Japan Atomic Energy Agency, Mukoyama, Naka, Ibaraki 311-0193, Japan

Abstract

A cyclic helium beam with energy 18.7 keV has been used to irradiate stress relieved and recrystallized powder metallurgy tungsten up to a fluence of $\sim 10^{23}$ He/m^2. After the helium irradiations, the samples have been exposed to pulsed high heat loading by an electron beam with a heat flux of 1 GW/m^2 and duration of 1, 1.5 or 2 ms. Surfaces of irradiated samples become smooth as a result of the electron beam irradiation of 1 GW/m^2 for 1 ms, due to atom migration on the surface at high temperature. On the other hands, the surface of irradiated samples is partially melted and resolidified. However, smoothing does not occur around the melted area. Stress relieved tungsten is melted by irradiation of a heat flux of 1 GW/m^2 and duration of 1.5 ms, but recrystallized tungsten is not melted by the same heat loading.

1. Introduction

The major fraction of ITER divertor armor is expected to be made of tungsten plates. Armor erosion and damage caused by high heat pulse loading due to disruptions and edge localized modes (ELMs) are critical issues for good performance of the tokamak. The armor is also subject to a high particle flux of hydrogen isotopes and helium from the plasma. This is a concern because it is well known that helium implanted in tungsten does not release until high temperatures, due to strong interaction with lattice defects [1]. Helium drastically enhances the formation of bubbles due to the strong bonding to vacancies and their clusters [2–7]. As a result, local swelling and degradation of mechanical properties of bulk materials take place [8].

As a basic study of the helium implantation effects, microstructure evolution during helium implantation has been investigated in metals under various irradiation conditions. Post irradiation annealing experiments have also been carried out to elucidate the thermal stability of defect clusters and their release behavior [9,10]. In addition, high heat loading experiments with helium particle beam have been performed. The result was that the loaded samples showed noticeable surface microstructure changes, such as blistering, exfoliation and a peculiar morphology [11]. It is clear that migration and coalescence of the helium bubbles play an essential role in the formation of such modification. It is also

* Corresponding author. Tel.: +81 92 583 7986; fax: +81 92 583 7690.
E-mail address: tokunaga@riam.kyushu-u.ac.jp (K. Tokunaga).

0022-3115/$ - see front matter © 2007 Elsevier B.V. All rights reserved.
doi:10.1016/j.jnucmat.2007.03.171

anticipated that implanted helium influences the response of tungsten to pulsed high heat loading. Very little information is available on the combined effects of helium implantations and the pulsed high heat loading. In the present work, helium pre-implanted tungsten has been exposed to pulsed electron beams to examine synergistic effects of helium implantation and pulsed high heat loading.

2. Experimental

Tungsten samples used in the present experiment are stress relieved and recrystallized material made by powder metallurgy tungsten by A.L.M.T. Corp. They were prepared by sintering followed by warm-rolling with a rolling thickness reduction of 80% with intermediate heat treatments. The first type of the sample was prepared by stress-relief (SR) annealing at 1473 K for 1.8 ks. The second type was obtained by recrystallization (RX) annealing at 1573 K for 3.6 ks. The sample sizes and purity are $20\ mm \times 20\ mm \times 5\ mm$ and 99.99%, respectively. The sample surface was mechanically and electrochemically polished.

Helium beam irradiations were performed in an ion beam facility at JAEA, Particle Beam Engineering Facility (PBEF). The samples were mechanically mounted on a Cu holder which was actively water cooled. The helium energy was 18.7 keV and its half width value was 140 mm. The helium beam flux and heat flux at the beam center was $2.0 \times 10^{21}\ He/m^2s$ and $6.0\ MW/m^2$, respectively. The beam duration was 2.8–3.0 s and interval between beam pulses was 27 s. The samples were irradiated to a fluence between 3.3×10^{23} and $5 \times 10^{23}\ He/m^2$ by 130–150 pulse irradiations cycles. The beam diameter on samples was 16 mm, defined using apertures. The surface temperature of the sample was measured with a two-color optical pyrometer and the two dimensional surface temperature distribution of the samples was also monitored with an IR camera. Temperatures of the samples were also measured with thermocouples on the side opposite the beam.

After the helium irradiation, the samples were exposed to pulse heat loading by electron beam irradiation using an Electron Beam Irradiation Stand (JEBIS) at JAEA. The heat flux was $1\ GW/m^2$, with duration of 1, 1.5 or 2 ms. The half width value of the electron beam was 8 mm. The electron beam area on the tungsten surface was defined by a beam limiter with an aperture of 4 mm. The net electron current induced by the electron beam irradiation was also measured, the electron beam energy was 70 keV, and the heat flux was measured by the calorimetric method. Before and after the helium and electron beam irradiation, the sample surfaces were examined using a scanning electron microscope (SEM). Sample weight loss was also measured.

3. Results and discussion

3.1. Surface modification by helium irradiation

The temperature evolution during a helium beam irradiation is shown in Fig. 1. The surface temperatures gradually increase, reaches a peak temperature, then starts to decrease after the beam is turned off. Surfaces are modified by blistering, sputtering and exfoliation. These modifications depend on fluence and peak temperature. Details of the surface modification due to the helium beam irradiation have already been reported [11].

3.2. Surface modification of helium irradiated tungsten after high heat pulse loading

Table 1 shows the conditions of electron beam irradiation. Shown in Fig. 2 are SEM images taken from the surface of stress relieved tungsten after electron beam irradiation. The sample in (a) was not irradiated before electron bombardment; sample (b) was helium irradiated before electron bombardment. The absorbed power density was $1\ GW/m^2$ for a duration of 1 ms. Small cracks formed on the electron beam irradiated surface area on each samples. In the case of the unirradiated

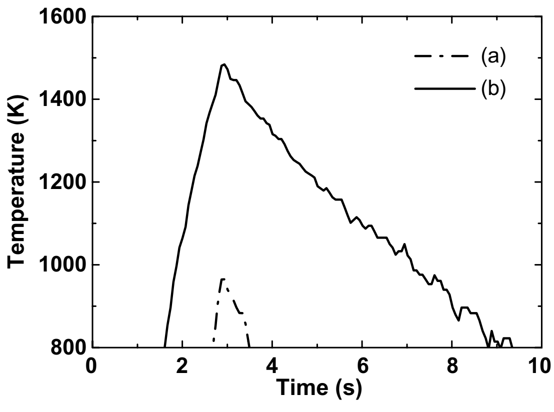

Fig. 1. Time evolution of surface temperatures measured by IR camera. Beam duration is 3.0 s. (a) $6.7 \times 10^{20}\ He/m^2s$ and (b) $1.0 \times 10^{21}\ He/m^2s$.

Table 1
Conditions of electron beam irradiations

Heat flux (GW/m^2)	1	1	1
Duration (ms)	1.0	1.5	2.0
Cyclic times	1, 10	1	1

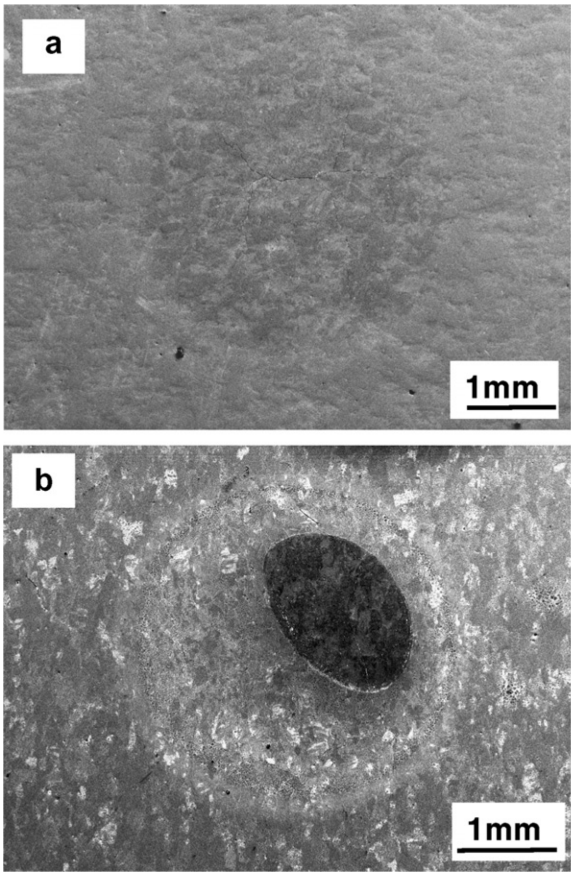

Fig. 2. SEM images taken from the surface irradiated by an electron beam with a heat flux of 1 GW/m^2 and a duration of 1 ms. (a) Stress relieved tungsten, unirradiated before electron bombardment and (b) stress relieved tungsten irradiated with 3.3×10^{23} He/m^2 at a peak temperature of 973 K, then electron bombardment.

sample, the surface became smooth as shown in Fig. 3. This is believed to be due to the migration of atoms near the surface at high temperatures.

In the case of the sample irradiated by helium, a part of the surface is melted and resolidified as shown in Fig. 2(b). Calculation of the depth profile of implanted helium by TRIM-code shows that helium atoms and primary damage are mostly concentrated near the surface and distributed up to 150 nm and 120 nm in depth, respectively. This

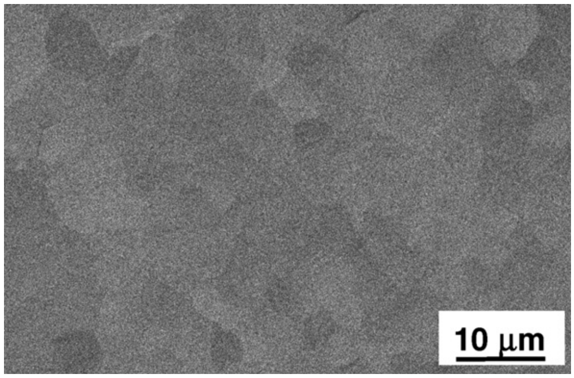

Fig. 3. SEM image taken from the surface of stress relieved tungsten irradiated by the electron beam with a heat flux of 1 GW/m^2.

means radiation damage, including bubbles formed in the near-surface region. As a result of the formation of the bubbles, decrease of thermal conductivity near the surface may allow melting by high heat pulse loading.

Shown in Fig. 4 are higher magnification SEM images of (a) boundary of melted and non-melted zone and (b) non-melted area. In the boundary zone, formation of blisters, exfoliation and small pin hole are observed as shown in Fig. 4(a). These surface modifications are considered to be due to the formation, coalescence and migration of helium bubbles near the surface during the pulse high heat loading of 1 ms. In addition, the pin holes may be formed by the migration of helium bubbles to the surface at a high temperature. On the other hand, surface smoothing did not occur; however, partial exfoliation of blister caps with a diameter of about 1 μm and cracks along grain boundaries are formed in the non-melted zone on the electron beam irradiated area, as shown in Fig. 4(b). It is possible that helium implantation in tungsten suppresses the migration of atoms at high temperature because radiation damage, such as helium bubbles act as obstacle to the atom migration.

After the 10th cyclic electron beam irradiation, surface smoothing much more appeared on the sample not previously irradiated by a helium beam. In addition, cracks grow and width of cracks increased on further repeated heat loadings. In the case of the helium irradiated sample, cracks also grow; however, there is little difference between the samples irradiated cyclically or by only one electron beam pulse. In the case of the recrystallized samples, the thermal behavior is almost the same;

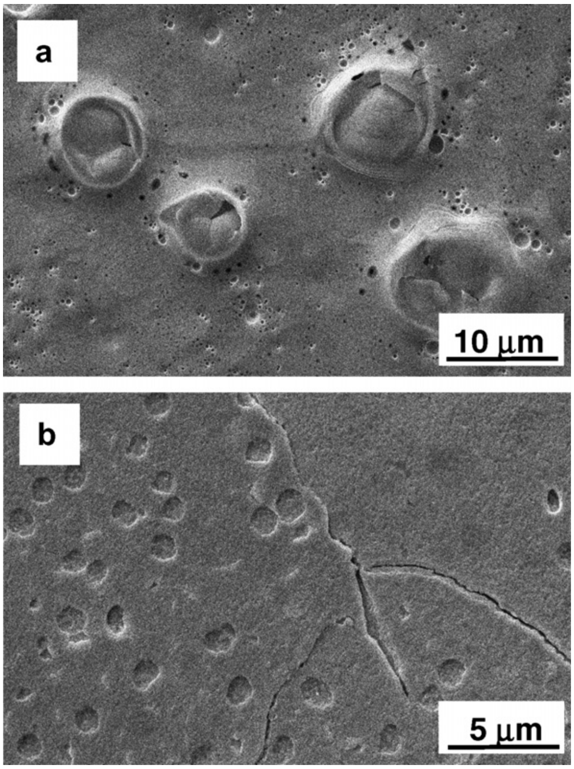

Fig. 4. SEM images taken from the surface irradiated by an electron beam with a heat flux of 1 GW/m^2 and a duration of 1 ms. Sample is stress relieved tungsten irradiated with 3.3×10^{23} He/m^2 at the peak temperature of 973 K before the electron bombardment. (a) Boundary between melted and un-melted zone and (b) un-melted area irradiated by the electron beam.

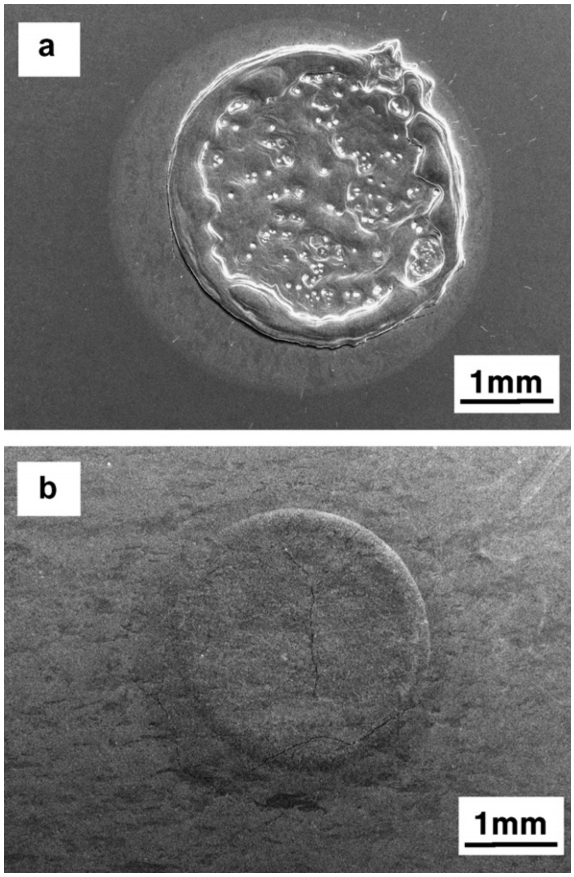

Fig. 5. SEM images taken from the surface irradiated by the electron beam with a heat flux of 1 GW/m^2 and a duration of 1.5 ms. (a) Stress relieved tungsten and (b) recrystallized tungsten.

however, the pattern of cracks is different compared to the stress relieved samples.

In the case of longer pulse heat loading, there is a difference in surface modification between the stress relieved and recrystallized samples which were not irradiated by the helium beam. Fig. 5 shows the SEM images of the stress relieved (a) and recrystallized (b) samples after irradiation by an electron beam with a heat flux of 1 GW/m^2 and a duration of 1.5 ms. In the case of the stress relieved sample, the surface has been melted and splashing of the melted layer occurred as shown in Fig. 5(a). On the other hands, in the case of the recrystallized sample, surface smoothing and flattening occurs but melting and splashing are not observed on the melted surface as shown in Fig. 5(b). Imamura has measured thermal conductivities of the samples by laser flash method. According to his results, the thermal conductivity of the recrystallized samples is about 5% larger than that of the stress relieved samples in the temperature range from RT to 1000 K [12]. This good thermal conductivity is believed to reduce the temperature increase of the recrystallized sample during the pulse heat loading.

Fig. 6 shows an SEM image of the stress relieved sample irradiated by the helium beam, then bombarded by an electron beam of power 1 GW/m^2 and a duration of 1.5 ms. The surface is melted, however, splashing of a melt layer is not observed and the sample has a smooth surface. Behavior of this modification is similar to that of the recrystallized samples irradiated by helium beam. Implanted helium may influence both the surface tension and viscosity of the melted layer because these physical properties affect the movement of molten metal. In addition, the lack of splashing may be due to the presence of helium bubbles at the grain boundaries or radiation defects before melting caused by the

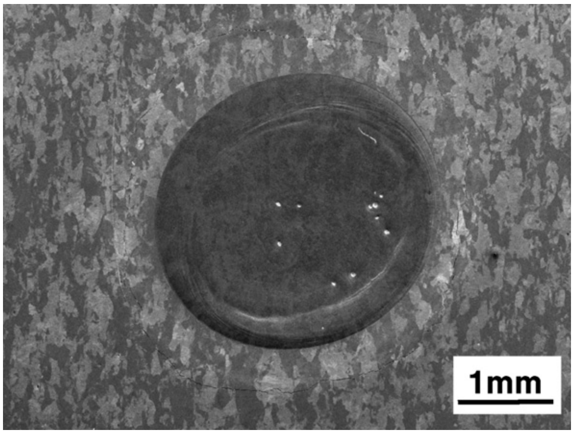

Fig. 6. SEM images taken from the surface irradiated by the electron beam with a heat flux of 1 GW/m^2 and a duration of 1.5 ms. Sample is stress relieved tungsten irradiated by 5.0×10^{23} He/m^2 at a peak temperature of 1473 K before the electron bombardment.

prior helium implantation that can affect the temperature gradient near the surface. In the case of further longer pulse heat loading, a duration of 2 ms and heat flux of 1 GW/m^2, all of the samples are melted and splashing of melt layer occurred.

4. Conclusion

Helium implantation influences the damage and erosion behavior of tungsten during pulsed high heat loading. Up to now, an electron beam has been mainly used as heat source for simulation experiments to investigate damage due to disruptions and Giant ELMs. However, the surface of divertor armor will be subjected to bombardment by helium as well as hydrogen isotopes, electrons, electromagnetic waves, X-rays, etc. Therefore, it is necessary to evaluate the damage and erosion effects caused by helium pre-implantation. In addition, the microstructure of tungsten is of importance because thermal properties depend on the microstructure.

References

[1] V.N. Chernikov, A.P. Zakharov, J. Nucl. Mater. 165 (1989) 89.
[2] M. Kaminsky (Ed.), Radiation Effects on Solid Surface, American Chemical Society, 1976, p. 112.
[3] H. Ullmaier, Radiat. Eff. 78 (1983) 1.
[4] B. Emmoth, Radiat. Eff. 78 (1983) 365.
[5] R. Behrisch, B.M.U. Scherzer, Radiat. Eff. 78 (1983) 393.
[6] V.N. Chernikov, Ju.V. Lakhotkin, H. Ullmaier, H. Trinkaus, P. Jung, H.J. Bierfeld, J. Nucl. Mater. 212–215 (1994) 375.
[7] P.B. Johnson, D.J. Mazey, J. Nucl. Mater. 218 (1995) 273.
[8] K. Shinohara, A. Kawakami, S. Kitajima, Y. Nakamura, M. Kutsuwada, J. Nucl. Mater. 179–181 (1991) 246.
[9] W.Th.M. Buters, A. Van der Beukel, J. Nucl. Mater. 141–143 (1986) 253.
[10] W.Te.M. Buters, A. Van Veen, A. Van der Beukel, Phys. Status Solidi (a) 100 (1987) 87.
[11] K. Tokunaga, S. Tamura, N. Yoshida, K. Ezato, M. Taniguchi, K. Sato, S. Suzuki, M. Akiba, J. Nucl. Mater. 329–333 (2004) 757.
[12] Imamura, private communication.